Theoretical determination of molecular structure and conformation. II. Hydrogen trioxide—a model compound for studying the conformational modes of geminal double rotors and five membered rings

D. Cremer

Lehrstuhl für Theoretische Chemie, Universität Köln, D-5000 Köln 41, West Germany
(Received 21 June 1978)

The internal rotational surface of hydrogen trioxide has been calculated with the Hartree–Fock method using basis sets with and without polarization functions and optimizing all structural parameters. These calculations have been repeated at the level of Rayleigh–Schrödinger–Møller–Plesset (RS–MP) perturbation theory in order to study the role of correlation effects on barrier values and structures. The relative energies as well as the computed geometrical parameters underline the importance of polarization functions. Although the intrapair correlation contributions significantly stabilize the planar conformations of H_2O_3, the net effect of correlation effects on the conformational potential is moderate because of well-balanced interpair contributions of opposite sign. As in the case of H_2O_2, the correlation effect on the relative energies further decreases if the basis set is improved. On the other hand, reliable structural parameters can only be achieved at the RS–MP level by employing a large augmented basis. The calculated equilibrium RS–MP structural parameters of H_2O_3 are: $R(OO) = 143.9$ pm, $R(OH) = 97.2$ pm, $\alpha(OOO) = 106.3°$, $\beta(OOH) = 100.2°$, $\theta = 78.1°$. Bond angles and OO bond lengths are strongly coupled to the rotational angles. A simultaneous rotation of both OH bonds is hindered by large barriers of 22.5 and 11.5 kcal/mole. These potential maxima can be surrounded in a stepwise flip-flop rotation of the OH groups. The barriers of this rotational process turn out to be the saddlepoint energies (6.5 and 5.4 kcal/mole) of the internal rotational surface. It is shown that a close relationship exists between the flip-flop rotation of the geminal double rotor and the pseudorotation of five membered rings. Using the calculated conformational potential $V(\theta_1,\theta_2)$, the prediction is made that the envelope form of 1,2,3-trioxolane is more stable than the corresponding twist form.

I. INTRODUCTION

The simplest molecular double rotor is hydrogen trioxide, the third member of the homologous series of hydrogen polyoxides beginning with H_2O and H_2O_2. In recent years interest in hydrogen polyoxides has increased due to the positive identification of the long postulated species H_2O_3 and H_2O_4[1] and the isolation of alkylated derivatives such as $(CH_3)_3COOOC(CH_3)_3$[2] and CF_3OOOCF_3.[3] In addition, H_2O_3 has been found to act as a hydroxylating agent in the superacid medium, thus opening new methods of organic synthesis.[4] Organic trioxides have been postulated to be intermediates in the ozonization of a variety of organic substrates.[5] Nevertheless, the extreme reactivity of H_2O_3 has prevented any deeper insight into its molecular structure and its conformational behavior. However, theory does not have to struggle with the limitations of experiment and can provide needed accurate data on H_2O_3 if the various effects of the type of theoretical model employed are carefully taken into consideration.

Apart from a more general chemical interest in H_2O_3, the actual objectives of this study are threefold. First, we want to investigate changes in electronic structure due to the incorporation of an oxygen atom in the OO linkage of hydrogen peroxide. Obviously, an accumulation of oxygen atoms in immediate or close vicinity leads to dramatic effects on structure, conformation, and stability which are normally explained by enhanced lone pair repulsion. This is related to the *anomeric* or *rabbits-ear effect*.[6] Secondly, a systematic evaluation of the conformational profile of H_2O_3 promises to provide a simple way to gain knowledge about the coupling mechanism between the individual rotors. Certainly, the electronic peculiarities of a rotating hydroxyl group influence the conformational tendencies of H_2O_3. This has to be analyzed in order to come to more general conclusions concerning the rotation of double rotors. Finally, H_2O_3 provides a useful model compound for 1,2,3-trioxolanes which have been postulated as intermediates in the ozonolysis of olefines.[7] Various predictions with regard to the conformation of these five membered rings have been made in order to explain the stereochemical course of the ozonolysis reaction. A complete knowledge of the conformational potential of H_2O_3 should be helpful in understanding the nature of 1,2,3-trioxolanes.

So far, only three limited *ab initio* studies of H_2O_3 have been reported in the literature,[8–10] all of them at the Hartree–Fock (HF) level of theory. They employed small or medium sized basis sets of the minimal,[8,10] split valence[8,9] or double-zeta[9] type to describe the rotational minimum of the molecule. While Radom *et al.*[8] used standard geometries in their calculation of H_2O_3, partial optimization of the geometrical parameters has been undertaken by Ažman *et al.*[10] (bond angles) and Newton *et al.*[9] (bond angles plus OO distance). However, a complete structure determination at the HF level is still missing, not to speak of a systematic exploration of the conformational surface. Furthermore, the question of whether polarization functions play an equally important role in HF calculations on H_2O_3 as they do

 0021-9606/78/6910-4456$01.00

for H_2O_2 has not been investigated previously. Also, no correlation corrected *ab initio* study of H_2O_3 has been reported.

In order to deal with these questions we have calculated distinct points of the conformational surface with various basis sets ranging from the minimal STO-3G basis to an optimum scaled augmented basis of 67 contracted Gaussian type functions (GTF). In addition, the conformational surface has been explored as a function of two rotational angles using a 60° grid. For each H_2O_3 conformation all geometrical parameters have been optimized. This procedure has been repeated with the Rayleigh–Schrödinger (RS) perturbation theory in order to correct energies and structures for possible correlation errors.

In Sec. III, the results of our *ab initio* calculations are discussed with regard to the predictions of various simple molecular orbital (MO) models of H_2O_3. In Sec. IV, the computed structural and conformational details of H_2O_3 are compared with those of H_2O_2. Sections V and VI deal with the basis set and correlation effects found for the various conformations of H_2O_3. Next, the form of the internal rotational potential is analyzed in Sec. VII, using various Fourier expansions. In Sec. VIII, possible modes of internal rotation are investigated with the aid of the computed energy contour map. A comparison with the pseudorotation of five membered rings is made. In specific, a parallel is drawn between the conformational tendencies of H_2O_3 and 1,2,3-trioxolane. Finally, in Sec. IX, common features of the conformational behavior of $X(OY)_2$ molecules are discussed.

II. COMPUTATIONAL DETAILS

As in the first paper of this series[23] we have used standard restricted Hartree–Fock (RHF) theory for closed shell molecules.[11] In order to make an assessment of the true HF energy of H_2O_3 the augmented $(9s5p1d/4s1p)[4s3p1d/2s1p]$ basis set of Dunning[12] has been employed. In paper I, optimum scale factors have been reported for this basis using H_2O_2 as a reference molecule. Results of this rescaled version of Dunning's contracted GTF basis (henceforth called Basis D) are compared with those of three other basis sets, namely A, B, and C: Basis A and B are Pople's minimal STO-3G[13] and split valence $[3s2p/2s]$ basis sets.[14] Basis C is also a split valence basis which is augmented by six $3d$ GTF's thus giving a $[3s2p1d/2s]$ basis.[15]

Correlation effects have been evaluated by the Møller–Plesset (MP) version of the Rayleigh–Schrödinger (RS) perturbation theory.[16] Second order RS–MP energies provide a reasonable estimate of correlation energies. They can be compared with the results of CI calculations including all double substituted configurations.[17]

All calculations have been performed with the program COLOGNE 76 which is a modified and improved version of GAUSSIAN 70.[18] COLOGNE 76 allows the efficient optimization of geometrical parameters with a quasi-Newton algorithm.[19] Structural parameters thus obtained are accurate to 0.2 pm and 0.2°.

III. RELATIVE STABILITIES OF DISTINCT CONFORMATIONS OF H_2O_3

Tables I and II summarize RHF energies and structures of seven distinct H_2O_3 conformations which are located at minima, maxima, and saddlepoints of the two-dimensional $E(\theta_1, \theta_2)$ surface. For all basis sets considered, the planar forms with *syn*-periplanar (sp) or *anti*-periplanar (ap) OH groups correspond to conformational maxima while those conformations with at least one OH

TABLE I. Absolute and relative RHF energies of minima, maxima, and saddlepoints of the conformational surface of H_2O_3.

Point	Conformation (symmetry)	Basis A STO-3G	Basis B $[3s2p/2s]$	Basis C $[3s2p1d/2s]$	Basis D[a] $[4s3p1d/2s1p]$
Absolute Energies (hartree)					
GMIN	+og, +og (C_2)	−222.58049	−225.21862	−225.53362	−225.61584
GMAX	sp, sp (C_{2v})	−222.54870	−225.18458	−225.49801	−225.58183
LMIN	+og, −og (C_s)	−222.57684	−225.21090	−225.52809	
LMAX1	ap, ap (C_{2v})	−222.57054	−225.20516	−225.51666	−225.60046
LMAX2	sp, ap (C_1)	−222.56846	−225.20740	−225.51729	
$S1$[b]	sp, +og (C_1)	−222.57167	−225.20944	−225.52273	
$S2$[b]	+og, ap (C_1)	−222.57563	−225.21193	−225.52560	
Relative energies (kcal/mole)					
GMIN	+og, +og (C_2)	0.0	0.0	0.0	0.0
GMAX	sp, sp (C_{2v})	19.9	21.4	22.3	21.3
LMIN	+og, −og (C_s)	2.3	4.8	3.5	
LMAX1	ap, ap (C_{2v})	6.2	8.5	10.6	9.6
LMAX2	sp, ap (C_1)	7.5	7.0	10.2	
$S1$[b]	sp, +og (C_1)	5.5	5.8	6.8	
$S2$[b]	+og, ap (C_1)	3.0	4.2	5.0	

[a]Geometrical parameters obtained with basis C have been used. The effect of rescaling[23] amounts to 0.00277 (GMIN), 0.00287 (GMAX), and 0.00429 hartree (LMAX1).

[b]Saddlepoint energies have been approximated for basis A and B, by setting $\theta_1(S1) = 0°$ and $\theta_2(S2) = 180°$, respectively, and optimizing the remaining geometrical parameters. In the case of the basis C, the rotational angles have been taken from the Fourier analysis described in Sec. VII.

TABLE II. Geometrical parameters of H_2O_3 obtained at the HF level with basis sets A, B, and C (bond lengths in pm, angles in degrees).

Parameter	GMIN C_2	GMAX C_{2v}	LMIN C_s	LMAX1 C_{2v}	LMAX2 C_1	$S1$[a] C_1	$S2$[a] C_1
Basis A, STO-3G							
θ_1	84.2	0.0	96.0	180.0	0.0	0.0	84.1
θ_2	84.2	0.0	−96.0	180.0	180.0	106.3	180.0
$R(O_1O_2)$	139.2	140.5	139.3	140.5	140.4	141.0	138.6
$R(O_2O_3)$					140.5	139.0	141.0
$R(O_1H)$	100.2	100.1	100.6	100.1	100.2	100.2	100.4
$R(O_3H)$					99.9	100.3	100.1
$\alpha(OOO)$	105.9	111.4	105.6	100.5	103.3	105.3	103.0
$\beta_1(HO_1O_2)$	102.5	105.1	101.1	99.0	102.3	102.0	102.5
$\beta_2(HO_3O_2)$					100.1	102.3	99.1
Basis B [3s2p/2s]							
θ_1	83.5	0.0	88.5	180.0	0.0	0.0	77.2
θ_2	83.5	0.0	−88.5	180.0	180.0	117.4	180.0
$R(O_1O_2)$	143.7	146.5	143.9	145.3	144.9	145.8	142.2
$R(O_2O_3)$					146.6	144.9	146.7
$R(O_1H)$	95.9	95.9	95.9	95.9	96.2	96.2	95.9
$R(O_3H)$					95.8	95.9	95.9
$\alpha(OOO)$	106.0	113.1	106.2	101.0	102.8	105.1	103.6
$\beta_1(HO_1O_2)$	103.6	109.2	108.6	100.7	103.8	103.8	103.8
$\beta_2(HO_3O_2)$					102.8	103.5	101.3
Basis C [3s2p1d/2s]							
θ_1	80.1	0.0	93.6	180.0	0.0	−13.1	80.2
θ_2	80.1	0.0	−93.6	180.0	180.0	105.0	187.6
$R(O_1O_2)$	137.3	139.4	137.3	138.9	138.6	139.3	135.9
$R(O_2O_3)$					139.6	137.3	140.0
$R(O_1H)$	95.3	95.0	95.2	95.2	95.3	95.3	95.3
$R(O_3H)$					95.2	95.2	95.2
$\alpha(OOO)$	107.2	112.9	107.6	101.7	104.4	107.2	104.7
$\beta_1(HO_1O_2)$	103.2	108.1	104.4	100.3	103.6	103.7	103.5
$\beta_2(HO_3O_2)$					101.3	103.1	100.5

[a]See note b in Table I.

group in an orthogonal (og) position lead to a point of favorably low energy corresponding either to a surface minimum or a saddlepoint. The zero point of energy is taken to be the energy of the (og, og) form which sits at the global minimum (GMIN) of the conformational surface. A second point of low energy can be found for the (+og, −og) conformation representing a local minimum (LMIN) of $E(\theta_1, \theta_2)$. A global maximum (GMAX) and two local maxima (LMAX1 and LMAX2) of the conformational surface result from the (sp, sp), the (ap, ap), and the (sp, ap) conformation, respectively. Finally, the saddlepoints S_1 and $S2$ are occupied by the (sp, +og) and (+og, ap) forms of the H_2O_3 molecule. Because of the C_{2v} symmetry of the potential surface, each conformation shown in Fig. 1 possesses one or several symmetry equivalents. Within the section $-180° \leq \theta_1, \theta_2 \leq +180°$, a total of 25 points with the unique energy properties of the seven conformations of Fig. 1 can be found.

The existence of a (og, og) global minimum for H_2O_3 is rationalized on the same basis as that used to rationalize the structure of H_2O or the equilibrium conformation of H_2O_2. In the oxygen atom, the two singly occupied orbitals ($2p_x$ and $2p_z$) are at right angles to one

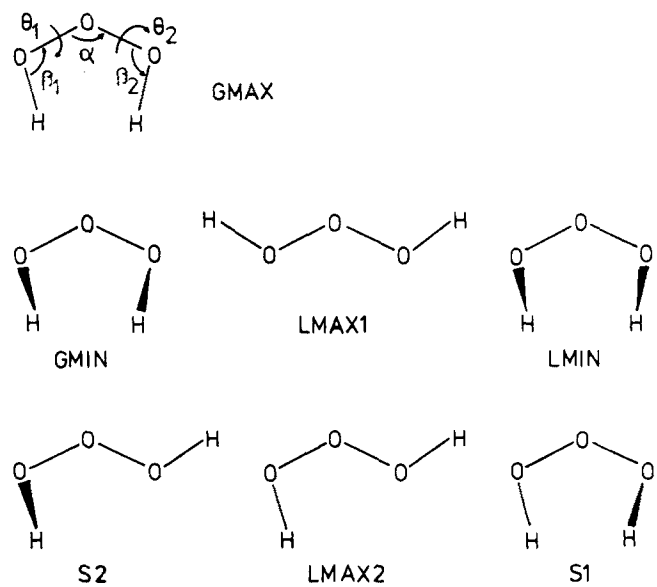

FIG. 1. The hydrogen trioxide conformations corresponding to the maximum, minimum or saddlepoint energies of the internal rotational potential. The definition of structural parameters is indicated.

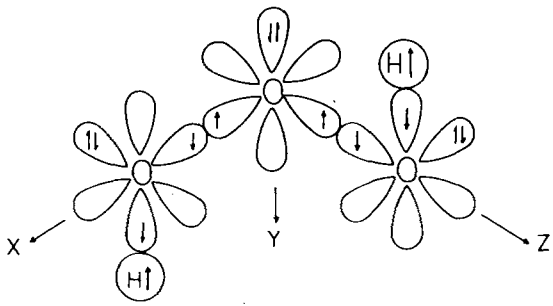

FIG. 2. Prediction of the most stable conformation of hydrogen trioxide by means of a simple bonding model.

another. Thus, to a first approximation the OOO angle in H_2O_3 will be 90°. To diminish lone pair repulsion between the O atoms, the free valences of the terminal O atoms point to the y direction. Hence, the OH bonds stand perpendicular to the OOO plane, being either on the same side or on opposite sides of the plane. A reduction of the H,H repulsion will lead to a preference of the (og,og) conformation (see Fig. 2). Those forms with two vicinal lone pairs in the same plane and the third in a plane perpendicular to the first one will be less favorable. Again, one can distinguish between a form with favorably low H,H repulsion, namely the (ap, +og) conformation, and one with higher H,H repulsion, namely the (sp, +og) conformation. A maximum of electron repulsion can be expected for those forms which have all oxygen lone pair orbitals perpendicular to the plane of the oxygen atoms. In this case, the energies will increase from the (ap,ap) to the (sp,sp) form according to a parallel increase of H,H repulsion.

With the aid of the simple bonding model used above, the relative stabilities listed in Table I are reproduced in a qualitative way.[20] In order to understand the structural details of H_2O_3, the perturbational molecular orbital (PMO) theory is adopted.[21] The PMO analysis of H_2O_3 involves a dissection of the molecule into component fragments, then, the construction of group orbitals (GO) for each fragment and, finally, an examination of the key GO interactions which arise in the recombination process of the fragments. Hydrogen trioxide can be dissected into two fragments, namely OH and OOH. In turn, the OOH fragment can be further dissected into O and a second OH group. Thus, there are two fragmentation modes and two sets of fragmentation orbitals upon which the PMO analysis can be based. Those group orbitals which are of primary interest for a dissection into O and the $(OH)_2$ group are schematically shown in Fig. 3. Recalling that the magnitude of the stabilizing or destabilizing GO interactions is largely determined by the size of the overlap we compare the interactions $p_y(O)-\pi_y$, $p_y(O)-\pi_y^*$, $p_y(O)-\pi_{x_+}^*$, and $p_y(O)-\pi_{x_-}^*$. Two of them, namely $p_y(O)-\pi_y^*$ and $p_y(O)-\pi_{x_-}^*$, can be excluded from the analysis because of zero overlap in all conformations. In a planar conformation, the interaction $p_y(O)-\pi_y$ will be destabilizing since two filled GO's interact. However, if the OH groups rotate, the destabilizing interaction of the overlap is reduced until it completely vanishes in an orthogonal conformation. Also, a stabilizing two electron interaction is possible between $p_y(O)$ and $\pi_{x_+}^*$ in the orthogonal conformation but not in the planar H_2O_3 forms. Hence, the conformational preference of skewed H_2O_3 forms over planar forms is accounted for by the PMO approach. Furthermore, it predicts shorter OO bond lengths for the orthogonal forms due to the additional overlap.

A similar result is obtained if the PMO analysis starts from a dissection into OOH and OH fragments. In Fig. 4, the GO's of hydroperoxyl and hydroxyl are depicted. They have been constructed from the corresponding H_2O_2 and H_2O MO's by removing the 1s contributions of one H atom. The double-head arrows, also drawn in Fig. 4, indicate those orbital interactions which become stabilizing ($\phi_6-\phi_6'$, $\phi_7-\phi_5'$, $\phi_8-\phi_5'$, $\phi_9-\phi_4'$, $\phi_9-\phi_6'$) or less destabilizing ($\phi_7-\phi_4'$ and $\phi_8-\phi_4'$) if the OH bond rotates out of the plane of the hydroperoxyl fragment.[22] Additional stabilization of a (sp, +og) or (ap, +og) form of H_2O_3 can result from interactions $\phi_9-\phi_3'$, and $\phi_6-\phi_7'$ where positive overlap between the p_y orbital of the central O atom and the 1s orbital of the hydroxyl hydrogen are possible. Besides a shorter OO bond length, a somewhat smaller OOH bond angle can be expected for the skewed forms.

Within the PMO approach, a distinction between the three planar forms is much more cumbersome since it requires reasonable estimates of overlap integrals and orbital energies for the analysis of almost a dozen possible interactions. Therefore, we refrain from a detailed PMO treatment, but utilize what is known from the quantum chemical study of hydrogen peroxide.[23] For example, the charge distribution in H_2O_2 indicates that the large electronegativity of the oxygen atom gives rise to a considerable bond dipole moment which is directed from the H atom (positive end) to the O atom (negative

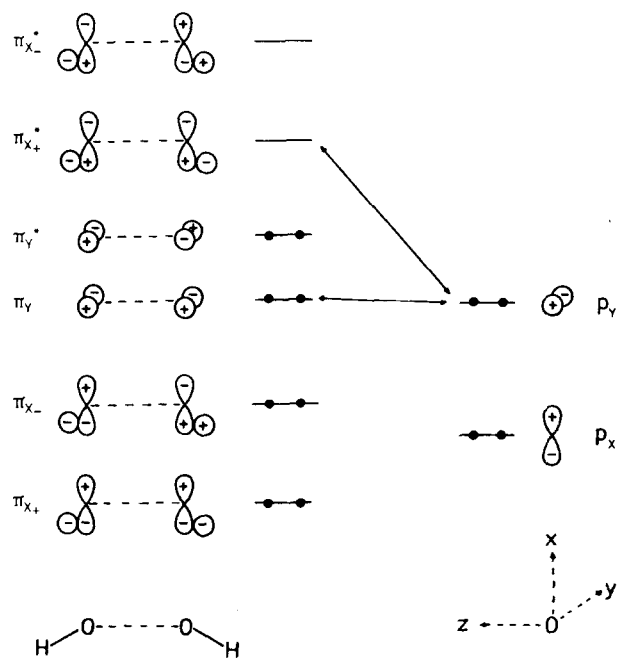

FIG. 3. Group orbitals which result from a dissection of H_2O_3 into O and $(OH)_2$. Stabilization of the orthogonal conformations arises from the interactions indicated by double-head arrows.

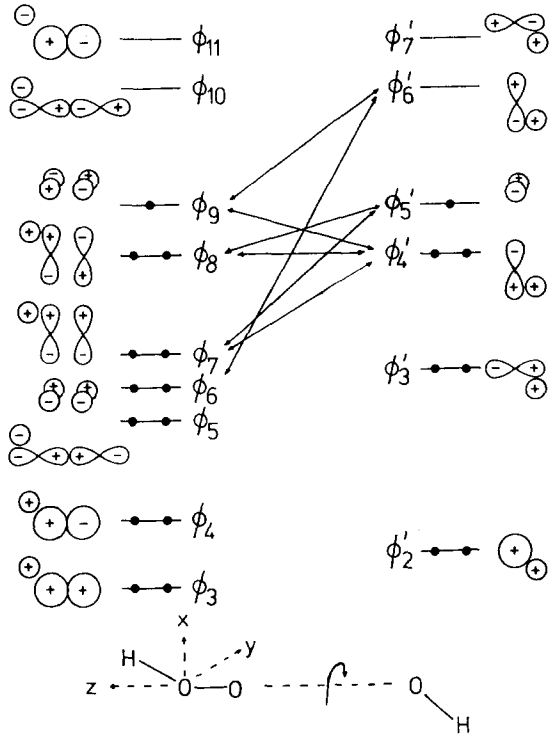

FIG. 4. The interaction of OOH and OH group orbitals in hydrogen trioxide. Interactions which become stabilizing or less destabilizing in a skewed position of the OH group are indicated by double-head arrows.

end). In the case of H_2O_3, we can describe the interaction of the two OH bond dipole moments approximately by Eq. (1)[24]:

$$E(DD)_{ab} = \frac{-\mu_a \mu_b}{r_{ab}^3} \times(+2\cos\omega_a\cos\omega_b - \sin\omega_a\sin\omega_b\cos(\tau_a - \tau_b)). \quad (1)$$

In Eq. (1) the magnitude of the dipoles μ_a and μ_b is determined by the charges on the O or H atoms and the distance l between these charges. The angles and distances are defined in Fig. 5. The dipole–dipole interaction is large and destabilizing if the distance r_{ab} is relatively small and the difference $\tau_a - \tau_b$ vanishes. The latter is true for the (sp, sp) and the (ap, ap) conformation, but not for the (sp, ap) conformation ($\tau_a - \tau_b = 180°$). The value of r_{ab} increases in the series (sp, sp), (sp, ap) and (ap, ap). Hence, the dipole–dipole interaction is highly unfavorable for the (sp, sp) form while the two other planar forms should be less destabilized, with the (sp, ap) form probably being slightly favored with regard to the (ap, ap) form. The destabilizing dipole–dipole interaction is further lowered if the OH bonds rotate in the (sc, sc), (og, og) or (ac, ac) positions, thus enlarging the values of the difference $\tau_a - \tau_b$ and of the distance r_{ab}. Compared with these conformations, the (+sc, −sc), (+og, −og) and (+ac, −ac) forms should be less favorable because of lower values of r_{ab} and $\tau_a - \tau_b$. Similarly, one can predict that the (og, ap) form is more stable than the (sp, og) form because the latter should imply a larger dipole–dipole interaction.

The application of Eq. (1) not only leads to a relative ordering of conformational energies, but also explains the more open structures of those H_2O_3 forms with strong dipole–dipole interactions. However, the variations in the OO bond lengths during rotation can be better described by a second quantum chemical effect, namely the tendency of lone pair electrons to delocalize in an adjacent polar bond. This effect was first described by Altona *et al.*[25] and later formulated in a more general way by Pople and co-workers.[26] It should cause a decrease of the OO bond length if the lone pair orbital of a terminal O atom is co-planar with the bond between the two other O atoms. This can happen in the orthogonal conformations, thus underlining the stability of these forms.

Usually, one refers to a third effect in order to analyze the behavior of alicyclic rotors. This is the concept of bond staggering which is also applied to molecules with lone pair electrons.[27] The latter are thought to be localized in sp^3 hybrid orbitals. Hence, rotational angles of 60° and 180° are the basic requirement for minimum lone pair repulsion and optimum OH bond staggering.

The computed energies and structures do not support this argument. At all calculational levels, the H_2O_3 conformations of low energy (GMIN and LMIN) are characterized by rotational angles close to 90°. Although the deviations from the perfectly orthogonal positions of the OH bonds, especially in the saddlepoint conformations, may arise from the tendency of lone pair staggering, this effect is certainly far less important than dipole–dipole interactions and lone pair delocalization.

IV. COMPARISON WITH H_2O_2

The theoretical energies and conformations of H_2O_3 listed in Tables I and II reveal its close relationship to hydrogen peroxide. Despite the similarity of structural and conformational parameters, there exist some differences:

(1) The OO bond lengths of H_2O_3 are shorter than that of H_2O_2 by 1–2 pm depending on the conformation considered. In the orthogonal conformations, lone pair delocalization into an OO bond is certainly more effective than into an OH bond. This becomes fairly obvious if Altona's[25] interpretation of this effect is adopted which is based on the mixing of one oxygen p orbital with the suitably oriented σ^* orbital of the OX bond (X = O or H). As the σ^*_{OH} orbital is usually higher in energy than the σ^*_{OO} orbital, orbital mixing will be more pronounced in

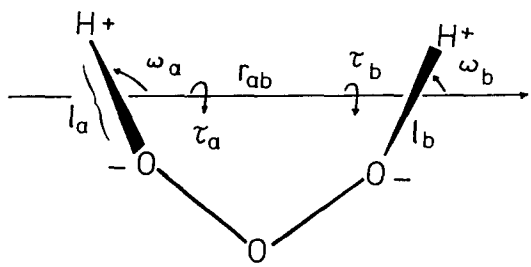

FIG. 5. The interaction of the two OH dipole moments in H_2O_3. The symbols refer to Eq. (1).

H_2O_3 than in H_2O_2. The consequences of this effect can be observed in the OO bond lengths obtained for the saddlepoint conformations (Table II). There, only one OO bond strengthens while the other OO bond is weakened due to the stronger participation of its σ^* orbital in the bonding process. As this weakening is not counterbalanced by a similar effect involving the σ^* orbital of the stabilized bond, the latter is shorter than those of the (+og, +og) form. Similarly, the longest OO bonds are found for the saddlepoint conformations rather than for the planar forms as one could expect.

(2) While the lone pair orbitals of the terminal oxygen atoms are mainly involved in an interaction with the σ^* orbital of the vicinal OO bond, those of the central O atom can interact with the OH bond, provided the lone pair orbital and the OH bond are coplanar. Again, this leads to a decrease of the corresponding OO bond and an increase of the OH bond length. It is not immediately clear why this effect should be larger for H_2O_3 than for H_2O_2 as suggested by the R(OH) values of 95.3 pm (H_2O_3 at equilibrium; RHF/basis C) and 94.6 pm (H_2O_2 at equilibrium, RHF/basis C). However, the equilibrium dihedral angles of 116° (H_2O_2) and 80° (H_2O_3) indicate that the interaction of an O lone pair orbital with the OH bond is stronger for H_2O_3 because of geometrical reasons. Consequently, the OH bond lengths of H_2O_2 and H_2O_3 are almost the same for the planar forms where this effect should play no significant role.

(3) Comparing the relative energies of H_2O_3 and H_2O_2 it becomes obvious that the barrier heights to internal rotation are not so strongly related as one could expect. The energy required to rotate H_2O_2 from the equilibrium conformation in the *syn* form is about 9 kcal/mole (RHF/basis C). A similar conformational process, namely (og, og) – (sp, og), requires about 7 kcal/mole if the same level of RHF accuracy is used. The difference of 2 kcal/mole is rather low if one recalls the interactions between different pairs of atoms (H ··· H vs H ··· O) and different bonds (OH and (H vs OH and OO) for H_2O_2 and H_3O_2. Another 15 kcal/mole are necessary to bring H_2O_3 to the (sp, sp) conformation where the large increase may result from strong H, H repulsion. However, if one analyzes the electron distribution in the (sp, sp) form with the aid of the Mulliken population values, it becomes obvious that the interaction between the H atoms is attractive, rather than repulsive. While the H, H overlap population is negligible or even antibonding in all other conformations, significant bonding overlap characterizes the (sp, sp) form. This suggests the same kind of "aromatic" stabilization due to σ-electron delocalization which was found for singlet dimethylcarbene.[28] Considering the atomic orbitals involved in the OH bonds as well as the in-plane lone pair orbital of the central O atom, then, a ring of five atomic orbitals can be formed which is closed by the H, H interaction. The assignment of six σ-electrons to the three resulting bonding MO's will lead to some stabilization of the *syn*-periplanar arrangement displayed in the positive H, H overlap population.

The σ-effect is partially offset by a destabilizing π-effect. Similar to the situation in the allyl anion, the planar H_2O_3 molecule possesses three π molecular orbitals, bonding, nonbonding, and antibonding. Since six electrons occupy these MO's the net effect leads to slightly destabilizing interactions between the O atoms according to the computed π overlap populations. Additional destabilization, of course, results from highly unfavorable dipole–dipole interactions.

The energy which is necessary to rotate one OH bond from the orthogonal position in the *anti*periplanar position amounts to 5 kcal/mole. It doubles if the second OH bond is brought in the same position. Since the same process for H_2O_2 takes less than 1 kcal/mole (RHF/basis C)[23] we can conclude that the trans arrangement of OO and OH bonds in H_2O_3 is less stable by more than 4 kcal/mole compared to H_2O_2. Probably, this is also caused by the unfavorable dipole–dipole interactions in the (ap, ap) and (ap, +og) forms of H_2O_3 which are not present in *trans* H_2O_2.

V. BASIS SET EFFECTS

The data compiled in Tables I and II indicate the basis set effects inherent in a RHF calculation of H_2O_3. In the case of H_2O_2 only augmented basis sets of the double-ζ-quality lead to a *trans* barrier to internal rotation, i.e., small basis sets are insufficient to describe the stabilization of skewed H_2O_2 relative to its *trans* form. This is also true for H_2O_3 as the saddlepoint energy of *S*2 (Table I) increases by 2 kcal/mole from a minimal basis set calculation to an augmented basis set calculation. This basis set effect also occurs with other conformations of H_2O_3. For the all-*trans* arrangement of bonds in the (ap, ap) form, the increase of energy due to basis set enlargement is twice as large, namely 4 kcal/mole.

In contrast to H_2O_2, the energies of the *syn*-periplanar forms of H_2O_3 increase with an improvement of the basis. The increase amounts to 1 kcal/mole for the (sp, +og) conformation and 2 kcal/mole for the (sp, sp) conformation. Also, the basis set effects found for the (+og, –og) and (sp, ap) forms are in line with energy increases of 1 and 2 kcal/mole for rotation in a *syn*- or *anti*periplanar form. We conclude that polarization functions are of similar importance for an accurate determination of the rotational barriers of H_2O_3 as they are for H_2O_2. With regard to the relative energies of the doubly augmented basis D, the same slight reduction of barrier heights exists as was found for H_2O_2.[23]

The actual basis set dependence is best found in the computed structures (Table II). The minimal STO-3G basis both underestimates the OO bond distances and overestimates the OH bond distances as a consequence of insufficient charge separation along the OH bond. Furthermore, the rigidity of the STO-3G basis leads to bond and dihedral angles close to 90°. Both effects contribute to the low *cis* and *trans* barriers obtained with the minimal basis A.

The structures obtained from basis set B show significant improvements. Due to its split valence shell character, basis B gives a relatively large separation of charge in the OH bonds which is responsible for the increase of the OO bond lengths, the decrease of the OH

TABLE III. Absolute and relative RS–MP energies of minima, maxima, and saddlepoints of the conformational surface of H_2O_3. Numbers in parenthesis are second-order correlation energies.

		Basis B		Basis C	
Point	Conformation (symmetry)	Total energy	(Corr. energy)	Total energy	(Corr. energy)
Absolute energies (hartree)					
GMIN	+og, +og (C_2)	−225.62077	(−0.41421)	−226.09075	(−0.56513)
GMAX	sp, sp (C_{2v})	−225.58952	(−0.41867)	−226.05486	(−0.56564)
LMIN	+og, −og (C_s)	−225.61327	(−0.41451)	−226.08511	(−0.56506)
LMAX1	ap, ap (C_{2v})	−225.60637	(−0.41578)	−226.07235	(−0.56511)
LMAX2	sp, ap (C_1)	−225.60940	(−0.41567)	−226.07358	(−0.56511)
$S1$[a]	sp, +og (C_1)	−225.61295	(−0.41707)	−226.08044	(−0.56643)
$S2$[a]	+og, ap (C_1)	−225.61352	(−0.41472)	−226.08222	(−0.56540)
Relative energies (kcal/mole)					
GMIN	+og, +og (C_2)	0.0	(2.8)	0.0	(0.8)
GMAX	sp, sp (C_{2v})	19.6	(0.0)	22.5	(0.5)
LMIN	+og, −og (C_s)	4.7	(2.6)	3.5	(0.9)
LMAX1	ap, ap (C_{2v})	9.0	(1.8)	11.5	(0.8)
LMAX2	sp, ap (C_1)	7.1	(1.9)	10.8	(0.8)
$S1$[a]	sp, +og (C_1)	4.9	(1.0)	6.5	(0.0)
$S2$[a]	+og, ap (C_1)	4.5	(2.5)	5.4	(0.6)

[a]Saddlepoint energies have been approximated for basis B by setting $\theta_1(S1) = 0°$ and $\theta_2(S2) = 180°$, respectively, and optimizing the remaining geometrical parameters. In the case of basis C, the rotational angles have been taken from the Fourier analysis described in Sec. VII.

bond lengths, and the opening of the bond angles. Although the computed structural parameters are of the magnitude expected for H_2O_3, they still differ significantly from the true HF values. This becomes clear if the overlap is improved by adding d functions to basis B. With basis C, the description of the OH bond polarity is over corrected by an increase of the OH overlap population. Consequently, a large augmented basis like C or D leads to bond distances shorter than the experimental equilibrium values. This is also true for H_2O_2[23] and results from an insufficient description of left–right electron correlation at the HF level of theory.[29]

VI. CORRELATION EFFECTS

In order to get an estimate of the correlation error we have repeated calculations with basis B and C at the RS–MP level of theory. RS–MP total energies, second order correlation energies, intra- and interpair contributions as well as computed structures are summarized in Tables III, IV, and V. While the basis B barriers are slightly reduced with respect to the RHF values the contrary is true for the basis C barriers. The latter is consistent with the increase of barrier heights found for H_2O_2 at the RS–MP level.[23] This increase results from a redistribution of charge from inner to outer shell regions due to the introduction of electron correlation. As a consequence, charge repulsion effects are somewhat larger, thus, leading to the higher barriers. It is interesting to note that the relative contributions of second order energies are about 1 kcal/mole smaller at the level of basis C than at level of basis B. Obviously, the observation[23] that correlation contributions to the H_2O_2 barriers become negligible if the basis set approaches the HF limit, also holds for H_2O_3.

In contrast to the total correlation energies, the intrapair and interpair portions (Table IV) significantly contribute to the relative conformational energies. The interpair correlation energy stabilizes the orthogonal forms while the intrapair energies favor the planar H_2O_3 conformations. Using the actual form of the molecular orbitals and the calculated electron distribution, it can be deduced that the lone pair MO's of the orthogonal conformations span nearly the whole region of the molecule. Therefore, the interaction of the lone pairs and the bond pairs is large which is in line with the predictions of the PMO treatment of H_2O_3. However, in the planar forms, the lone pair MO's do not span as much of the molecule. Hence, interpair interactions become less important while intrapair correlations become significant. The small net effect of the correlation energies on the barriers results from the well-balanced contributions of inter- and intrapair terms. As a consequence, the relative conformational energies of H_2O_3 can be determined at the HF level of theory with a reasonable degree of ac-

TABLE IV. Intra- and interpair energies of H_2O_3 obtained with basis C at the RS–MP level of theory. Absolute energies are given in hartree, relative energies (in parenthesis) in kcal/mole.

Point	Conformation	Intrapair energy	Interpair energy
GMIN	+og, +og (C_2)	−0.08360 (6.1)	−0.48154 (0.2)
GMAX	sp, sp (C_{2v})	−0.09213 (0.7)	−0.47351 (5.3)
LMIN	+og, −og (C_s)	−0.08316 (6.4)	−0.48190 (0.0)
LMAX1	ap, ap (C_{2v})	−0.08749 (3.6)	−0.47763 (2.7)
LMAX2	sp, ap (C_1)	−0.09331 (0.0)	−0.47179 (6.3)
$S1$	sp, +og (C_1)	−0.09015 (2.0)	−0.47628 (3.5)
$S2$	+og, ap (C_1)	−0.09033 (1.9)	−0.47507 (4.2)

TABLE V. Structural parameters of H_2O_3 as determined by second order RS–MP theory with basis sets B and C (bond lengths in pm, angles in degrees).

Parameter	GMIN C_2	GMAX C_{2v}	LMIN C_s	LMAX1 C_{2v}	LMAX2 C_1	S1[a] C_1	S2[a] C_1
Basis B [3s2p/2s]							
θ_1	78.3	0.0	92.2	180.0	0.0	0.0	76.0
θ_2	78.3	0.0	−92.2	180.0	180.0	108.7	180.0
$R(O_1O_2)$	153.9	157.6	154.0	156.4	155.2	157.2	151.3
$R(O_2O_3)$					158.3	155.1	158.8
$R(O_1H)$	99.2	99.3	99.2	99.4	99.6	99.6	99.1
$R(O_3H)$					99.1	99.2	99.2
α(OOO)	104.4	111.5	105.1	96.0	98.8	102.3	100.4
$\beta_1(HO_1O_2)$	99.6	104.6	101.7		99.3	98.4	99.7
$\beta_2(HO_3O_2)$					98.6	99.3	96.7
Basis C [3s2p1d/2s]							
θ_1	78.5	0.0	90.8	180.0	0.0	−14.0	78.7
θ_2	78.5	0.0	−90.8	180.0	180.0	102.6	185.2
$R(O_1O_2)$	144.2	147.0	143.9	146.4	145.6	147.3	141.2
$R(O_2O_3)$					147.5	144.0	148.9
$R(O_1H)$	98.0	97.7	98.1	98.1	98.1	98.0	98.1
$R(O_3H)$					98.0	98.0	98.4
α(OOO)	106.1	112.1	106.9	98.8	102.3	105.4	102.8
$\beta_1(HO_1O_2)$	100.3	105.3	101.2	96.8	100.4	99.7	101.2
$\beta_2(HO_3O_2)$					98.1	99.8	97.3

[a]See comment a in Table III.

curacy. Although this finding is in line with similar observations made for H_2O_2, it does not necessarily suggest that the relative interpair and intrapair contributions always cancel.

Unlike the barrier values, the computed RS–MP equilibrium structures of the seven H_2O_3 conformations (Table V) clearly differ from the corresponding RHF results. For both basis B and basis C, the bond distances become longer while the bond angles are slightly reduced. The RS–MP method uses all doubly substituted determinants Φ_{ij}^{ab} in the calculation of the second order energy[16] including double excitations from OO or OH bonding to OO or OH antibonding molecular orbitals. This allows for left–right correlation of the bond electrons. The corresponding contributions to the correlation energy are significant if the basis set provides low-lying virtual orbitals with the right nodal properties in the bond region. For basis B, these conditions are not fulfilled. Only, if the bond lengths are substantially increased from their HF values, is the gap between bonding and antibonding OO and OH MO's diminished and the contributions to the correlation energy arising from double excitations to σ^*_{OO}, π^*_{OO}, and σ^*_{OH} MO's become significant. Furthermore, the tendency of basis B to overestimate bond polarities influences the values of R(OO) and R(OH). As was already described for H_2O_2,[23] the inclusion of correlation effects causes a redistribution of charge from inner atomic to outer atomic regions. Consequently, charge repulsion is increased, thus leading to unreasonably long bond lengths of H_2O_3. To get reliable structural values an augmented basis like C is necessary which allows for sufficient left–right correlation of bond electrons. Any larger basis set than C should lead to a slight reduction of the bond lengths of Table V due to enhanced overlap. Especially, the R(OH) values should decrease as basis C does not include polarization functions on the hydrogens.

In order to give some verification for these predictions we have augmented basis C with three p GTF's for hydrogen[15] and have repeated the structure optimization of the conformation of lowest energy at the RS–MP level. The energy thus obtained amounts to −226.11275 hartree including a second order correlation energy of −0.57421 hartree. The theoretical equilibrium parameters are: R(OO) = 143.9 pm, R(OH) = 97.2 pm, α(OOO) = 106.3°, β(HOO) = 100.2°, and θ = 78.1°. It may be noted that the calculated value of R(OH) fits nicely in the series of theoretical OH bond lengths of H_2O (95.7 pm), H_2O_2 (96.7 pm), and HOF (97.2 pm) evaluated at the same level of accuracy.[30]

VII. THE INTERNAL ROTATIONAL POTENTIAL

Since the principal aim of this work is the investigation of the internal rotational potential surface of H_2O_3, we have calculated the analytical form of $E(\theta_1, \theta_2)$. For this purpose, a 60° grid was used covering the range $-180° \leq \theta_1, \theta_2 \leq +180°$. At each point, all bond lengths and bond angles have been optimized. In a first set of calculations, basis C was employed at the HF level of theory. Then, in a second set of calculations, the same conformations have been recalculated using basis C at the RS–MP level of theory. Again, all structural parameters have been optimized in order to get reliable predictions on correlation dependent changes of the conformational potential. The energies obtained in this way are listed in Table VI. The energy of GMIN is used as a reference, throughout.

TABLE VI. Conformational energies of H_2O_3 obtained with basis C at the HF and the RS–MP level. *Ab initio* values are compared with those of the Fourier analysis using Eq. (4). Angles are given in degrees, energies in kcal/mole relative to GMIN.

		RHF energies		RS–MP energies	
θ_1	θ_2	*ab initio*	Fourier[a]	*ab initio*	Fourier[b]
180.0	0.0	10.2	10.4	10.8	11.0
	60.0	5.8	5.8	6.1	6.0
	120.0	7.2	7.0	7.8	7.6
	180.0	10.6	10.6	11.5	11.6
120.0	−120.0	5.2	5.3	5.7	5.6
	−60.0	4.6	4.2	4.5	4.1
	0.0	7.1	7.0	6.9	6.8
	60.0	2.8	2.7	3.0	3.0
	120.0	3.9	4.2	4.4	4.8
60.0	−60.0	8.5	8.5	8.2	8.3
	0.0	11.0	11.5	10.4	11.1
	60.0	1.7	1.8	1.3	1.3
0.0	0.0	22.3	22.0	22.5	22.1
θ(GMIN)[c]	θ(GMIN)	0.0	−0.3	0.0	−0.3
θ(LMIN)[c]	θ(LMIN)	3.5	3.7	3.5	3.8

[a]Correlation coefficient $r^2 = 0.998$.
[b]Correlation coefficient $r^2 = 0.997$.
[c]The RHF values of θ(GMIN) and θ(LMIN) are 80.1° and 93.6°, respectively. The corresponding RS–MP values are 78.3° and 92.2°, respectively.

In general, the potential function of a single rotor can be reasonably approximated by the truncated Fourier expansion (2):

$$V(\theta) = \sum_{k=0}^{m} (V_k^c \cos k\theta + V_k^s \sin k\theta) \ , \qquad (2)$$

where m takes a finite value. The decomposition of the potential V into its Fourier components V_k facilitates the interpretation of the rotational barriers as has been shown by Radom *et al.*[26] The success of this approach makes it desirable to develop the potential of a multi rotor in a similar way. In the case of H_2O_3, the dependence of V on the rotational angles θ_1 and θ_2 can be written as

$$V(\theta_1,\theta_2) = \sum_{k=0}^{m}\sum_{l=0}^{n} (V_{kl}^{cc}\cos k\theta_1 \cos l\theta_2 + V_{kl}^{cs}\cos k\theta_1 \sin l\theta_2 + V_{kl}^{sc}\sin k\theta_1 \cos l\theta_2 + V_{kl}^{ss}\sin k\theta_1 \sin l\theta_2) \ . \qquad (3)$$

In order to reduce the numerous terms in Eq. (3) the summation limits $m = n = 3$ are chosen in accordance with the treatment of single rotors. Furthermore, all Fourier terms can be excluded which do not comply with the C_{2v} symmetry of the potential surface. The remaining terms have been systematically investigated by performing a least-squares analysis for a series of trial expansions of Eq. (3) using a total of 19 *ab initio* energies. According to the evaluated standard deviations σ and correlation coefficients r^2,[31] the best fit of the *ab initio* data has been achieved with Fourier expansion (4)[32]:

$$V(\theta_1,\theta_2) = V_{00} + \sum_{i=1}^{2}[\tfrac{1}{2}V_{10}(1-\cos\theta_i) + \tfrac{1}{2}V_{20}(1-\cos 2\theta_i) + \tfrac{1}{2}V_{30}(1-\cos 3\theta_i)] + V_{11}^{cc}\cos\theta_1\cos\theta_2 + V_{11}^{ss}\sin\theta_1\sin\theta_2 + V_{22}^{cc}\cos 2\theta_1\cos 2\theta_2 + V_{22}^{ss}\sin 2\theta_1\sin 2\theta_2 + V_{12}[\cos(\theta_1+2\theta_2)+\cos(2\theta_1+\theta_2)] \ . \qquad (4)$$

The V_{kl} coefficients of the RHF and RS–MP $V(\theta_1,\theta_2)$ surface of H_2O_3 are presented in Table VII together with the corresponding values of σ and r^2. The relative energies evaluated with (4) are shown in Table VI.

TABLE VII. Fourier analysis of the $V(\theta_1,\theta_2)$ rotational potential surface for various geminal double rotors of the $X(OY)_2$ type.

Molecule	H_2O_3[a] RHF/Basis C	H_2O_3[a] RS–MP/Basis C	$CH_2(OH)_2$[b] RHF/Basis B	$CH_2(OH)_2$[b] RHF/Basis C	$CH_2(OCH_3)_2$[c] RHF/Basis B	$H_2PO_4^-$[d] RHF/STO-3G	$(CH_3)_2PO_4^-$[e] RHF/STO-3G
V_{10}	−2.99	−2.31	2.78	1.76	−8.42	−0.44	−1.38
V_{20}	−5.67	−5.90	−1.73	−1.82	−5.60	−3.27	−3.23
V_{30}	−0.80	−0.84	−1.12	−1.11	−3.54	0.16	−0.65
V_{11}^{cc}	2.93	2.90	3.16	2.37	7.56	0.71	2.18
V_{11}^{ss}	−1.79	−1.68	−1.72	−1.14	−4.25	−0.29	−1.09
V_{22}^{cc}	0.87	1.05	0.72	0.69	1.54	0.11	0.36
V_{22}^{ss}	−0.79	−0.90	−0.62	−0.66	−2.69	−0.08	−0.49
V_{12}	0.95	1.03	0.77	0.59	2.41	0.12	0.47
σ	0.33	0.38	0.41	0.50	1.93	0.10	0.19
r^2	0.998	0.997	0.990	0.989	0.969	0.999	0.997
Ref.	This work	This work	Ref. 38	Ref. 39	Ref. 39	Ref. 40	Ref. 41

[a]All structural parameters are optimized (19 surface points).
[b]Standard geometries are used. Rigid rotation is assumed. (Basis B: 20 points; Basis C: 12 points).
[c]Standard geometries and rigid rotation assumed. The methyl groups are kept fixed to give overall C_{2v} symmetry of the θ_1, θ_2 surface. (12 surface points; the (sp, sp) form was not calculated.)
[d]The STO-3G structure of the conformational minimum is used for 13 independent surface points. Rigid rotation is assumed.
[e]Experimental geometries are used. Rigid rotation assumed. Energies are estimated from the θ_1, θ_2 map in Ref. 40 (14 surface points). C_{2v} symmetry of the $V(\theta_1, \theta_2)$ surface assumed.

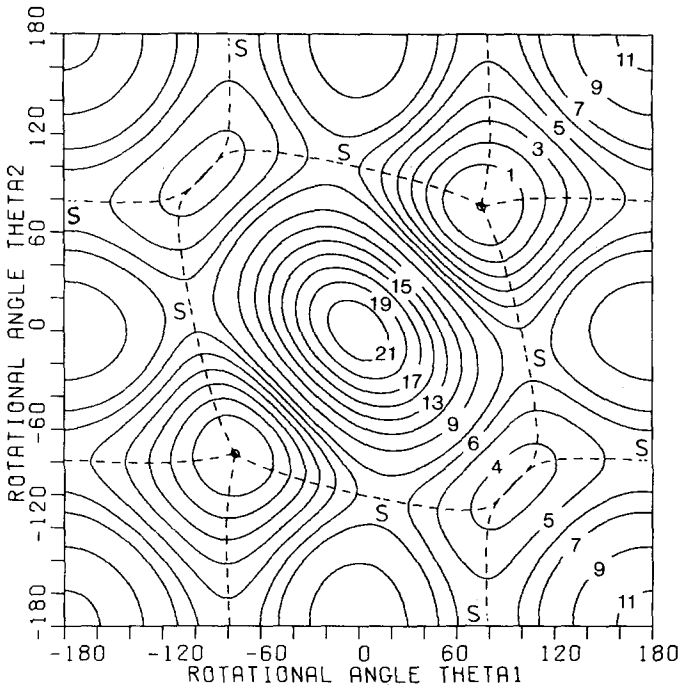

FIG. 6. The *ab initio* internal rotational potential for hydrogen trioxide (RS–MP/basis C), as a function of the dihedral angles θ_1 and θ_2. Contours indicate kcal/mole above the energy of GMIN. The dashed lines represent the steepest descent and ascent paths to and from the saddlepoints S.

As in the case of a single rotor, the magnitude of the V_{k0} terms illustrates the relative importance of dipole, hyperconjugative and bond staggering effect. According to the values of columns 1 and 2 of Table VII, the first and the second effect dominate the form of the potential while the influence of bond staggering is moderate. A similar observation can be made for the cross terms V_{kl} which describe the coupling of the three electronic effects. Fourier coefficients like V_{31} or V_{k3} have been found negligible in all trial calculations, also indicating the reduced importance of bond staggering. On the other hand, the values of V_{11}, V_{22}, and V_{12} are considerable arising from the influence of the dipole–dipole interactions, from the coupling between the hyperconjugative effects, and from the coupling between dipole and hyperconjugative effect. Since the interaction energy of two dipoles is proportional to $\cos(\tau_a - \tau_b)$ (see Eq. (1)) it seems reasonable to include a $\cos(\theta_1 + \theta_2)$ term in the Fourier expansion where the positive sign in the cosine argument results from the different definitions of τ_b and θ_2 (see Figs. 1 and 5). However, the angle ω_a and ω_b as well as the values of μ_a and μ_b, and the distance r_{ab} also vary with the rotational angles θ_1 and θ_2, thus leading to a more complicated dependence of the dipole–dipole interaction energy on θ_1 and θ_2 than that which is provided by a single cosine term. Therefore the cosine and sine part of the $\cos(\theta_1 + \theta_2)$ are separated in Eq. (4) to improve the description of the rotational potential.[33]

The positive sign of V_{11}^{cc} indicates that the (sp, ap) conformation is more stable than the other planar forms while the negative sign of V_{11}^{ss} indicates the preference of the (og, og) forms over the (og, −og) forms. The main features of the potential are reflected by the terms V_{10}, V_{20}, and V_{11} while second order effects which decide on the exact energies and locations of minima and saddlepoints can be extracted from the remaining terms of Eq. (4). The V_{22}^{cc} term, for example, leads to a stabilization of the saddlepoint conformations relative to the planar forms. Their location outside the 1st and 3rd but inside the 2nd and 4th quadrant of the θ_1, θ_2 coordinate system has to do with the negative sign of V_{22}^{ss} which also plays a role with regard to the position of GMIN and LMIN. An interplay of the negative V_{22}^{ss}, the negative V_{30}, and the positive V_{12} causes a shift of GMIN to θ values lower than 90° because all these terms favor the (sc, sc) forms. As for LMIN, these effects neutralize since V_{22}^{ss} stabilizes conformations close to $\theta_1 = \theta_2 = 135°$ which are destabilized by the V_{30} and V_{12} term.

Although none of the V_{12} or V_{21} terms of Eq. (3) complies with the symmetry restriction on $V(\theta_1, \theta_2)$, the inclusion of a cross term V_{12} proved to be necessary to give a satisfactory fit of the *ab initio* energies. It turned out that among the linear combinations of V_{12} terms with the right symmetry, the terms $(V_{12}^{cc} + V_{21}^{cc})$ and $-(V_{12}^{ss} + V_{21}^{ss})$ are most important where the sine part provides an efficient differentiation between the C_s and C_2 conformations of H_2O_3.[33] Without loss of accuracy, the two V_{12} components can be contracted to give the last term of Eq. (4).

Using the Fourier expansion $V(\theta_1, \theta_2)$, energy contour maps of the internal rotational potential of H_2O_3 have been plotted. The RS–MP rotational surface is shown in Fig. 6. One-dimensional sections out of this surface for $\theta_1 = 0°$, 60°, 120°, and 180° are displayed in Fig. 7. Both plots reflect the coupling between the OH rotors which is strongest for small rotational angles. For regions close to 180°, there appears to be some decoupling indicating similar dipole–dipole interactions for C_s and C_2 conformations that are almost planar.

Before discussing Fig. 6 in more detail, we would like to stress the correspondence between RHF and RS–MP Fourier coefficients (columns 1 and 2, Table VII). As was shown in Sec. VI, correlation effects change only slightly the barrier values due to the cancellation of intra- and interpair contributions. Surprisingly, it turns out that this conclusion also holds for the complete conformational potential. Contour maps of the intra- and interpair portions of the correlation energy shown in Figs. 8 and 9 are nearly the negatives of each. The form of the contours are almost identical in both plots, except that the maxima of the intrapair energies correspond to the minima of the interpair energies and vice versa. The location of these points is in line with our observation that the planar forms are stabilized by the intrapair contributions while the (og, og) and (og, −og) conformations are favored by the interpair contributions. Their net effect widely cancels giving rise to correlation contributions to the potential of 1–2 kcal/mole as shown in the contour map of relative correlation energies in Fig. 10. Although these values may decrease further with an improvement of the basis, two points can be made with regard to the dependence of correlation effects on the rotational angles. First, correlation effects are strongly coupled to θ_1 and θ_2. Secondly, the

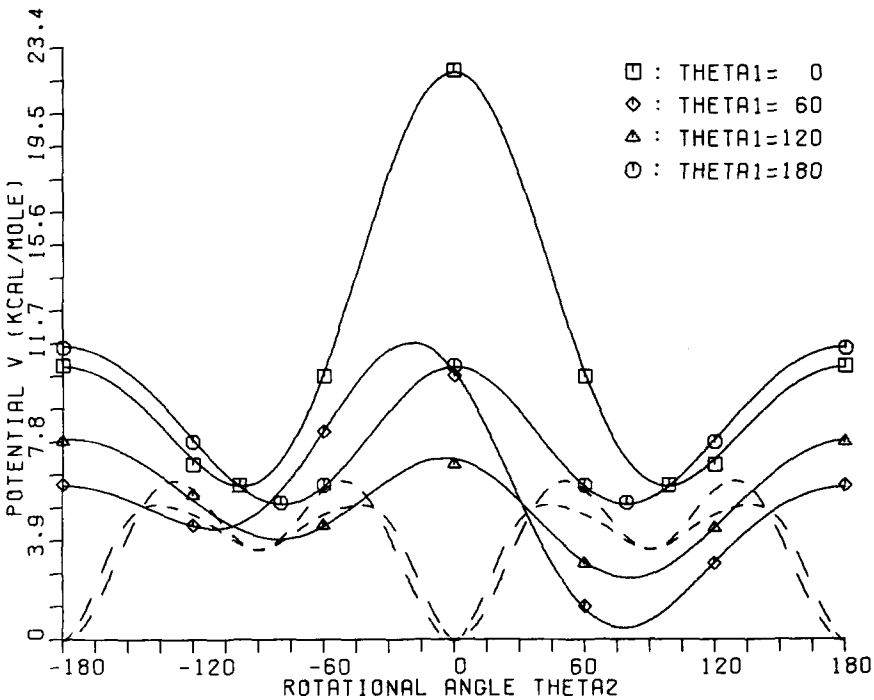

FIG. 7. Sections, $V(\theta_2)$, out of the potential surface for internal rotation of hydrogen trioxide for fixed values of θ_1. The dashed lines show the energy variation along the flip-flop rotational paths. They have been calculated by choosing polar coordinate systems centered at GMAX and LMAX1. The corresponding phase angles are defined to be 0° or 180° for the points GMIN and 90° or 270° for the points LMIN.

variation of the correlation energy is largest for conformational changes which preserve C_2 symmetry, i.e., along the left–right diagonal of Fig. 10, while it is relatively low for an internal rotation which preserves C_s symmetry, i.e., along the right–left diagonal. This is in line with the observation already made for the total energies of H_2O_3 and confirms that the electron rearrangement is more drastic for the symmetry retaining inversion of the (og, og) form than for the corresponding inversion of the (+og, −og) form.

VIII. THE FLIP-FLOP ROTATION OF THE DOUBLE ROTOR

With the aid of the energy contour map of H_2O_3, various rotational modes can be discussed. Synchronous rotation of both OH groups of the stable (og, og) form, either disrotatory or conrotatory, are prohibited by the large barriers at GMAX, LMAX1, and LMAX2. The two step rotations which are indicated by the dashed lines in Fig. 6 are more probable. They surround the con-

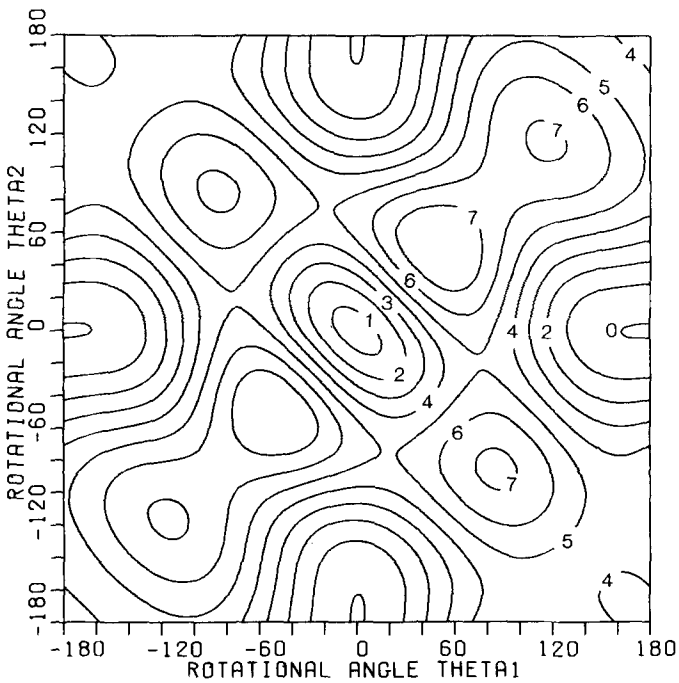

FIG. 8. The intrapair energies of hydrogen trioxide as a function of θ_1 and θ_2. Contours indicate kcal/mole above the intrapair energy of LMAX2.

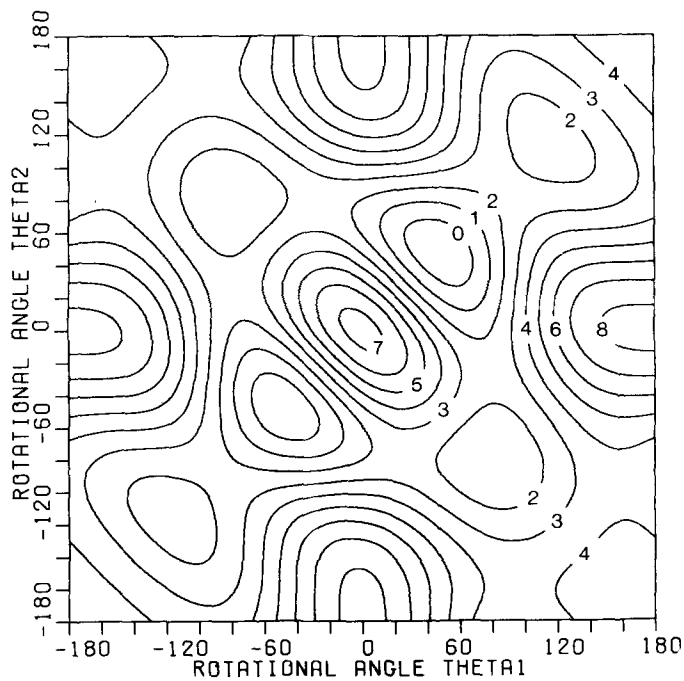

FIG. 9. The interpair energies of hydrogen trioxide as a function of θ_1 and θ_2. Contours indicate kcal/mole above the interpair energy of the (sc, sc) conformation of H_2O_3.

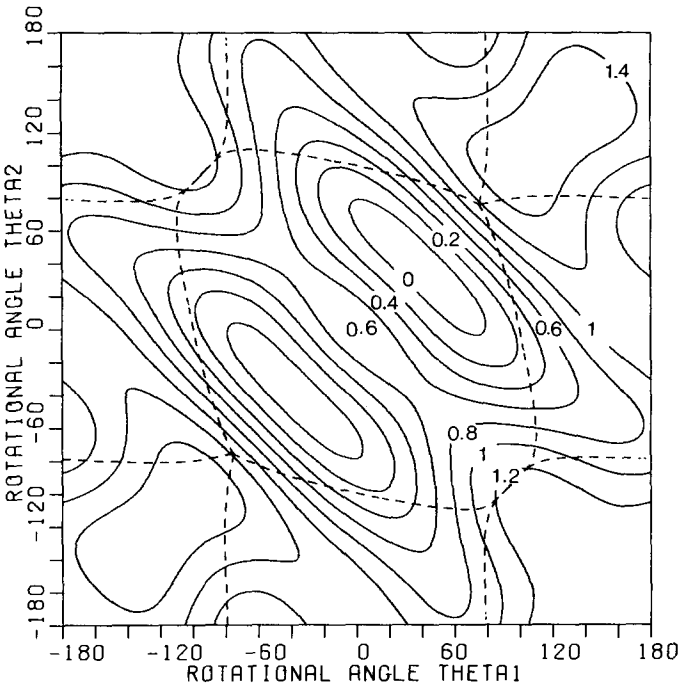

FIG. 10. Correlation energy contour map of hydrogen trioxide. Isoenergy contours are in kcal/mole above the conformation with the largest correlation energy ($\theta_1 = \theta_2 = 50°$). The dashed lines are transferred from Fig. 6 and indicate the paths of flip-flop rotation.

formational maxima by following the energy valleys of the θ_1, θ_2 surface which start at GMIN and end at one of the saddlepoints *S*1 or *S*2.[34]

If the molecule follows the closed path encircling GMAX, the first step of the conformational process consists of the inward rotation of one OH bond. First, the saddlepoint *S*1 (6.5 kcal/mole) is passed and, then, the rotation proceeds down to the local minimum LMIN. In the second step, the other OH bond also rotates inward. Now, the symmetry equivalent of *S*1 is surmounted and, after rotation by almost 180°, the symmetry equivalent of GMIN is reached. Repetition of this flop-flop rotation brings the molecule back to the starting point of the conformational process, thus surrounding GMAX in a less energy consuming manner than any other possible inward rotation of the OH bonds.

There is another unique rotational path indicated in Fig. 6. Following this path the H_2O_3 molecule surrounds the local energy maximum LMAX1. We describe the corresponding conversion as an outward flip-flop rotation hindered by the height of the barrier point *S*2 (5.4 kcal/mole). The combination of an inward and outward flip-flop rotation can lead to a path which encircles LMAX2. This rotation is characterized by two barrier values, namely those of *S*1 and *S*2.

The energy variation along the inward and outward flip-flop rotational paths is displayed by the dashed lines in Fig. 7. A twofold periodicity can be observed for a complete rotation. We note that the barrier heights of a flip-flop rotation of H_2O_3 are lower by 1–2 kcal/mole) than the *cis* barrier of H_2O_2.

At this point, it is interesting to compare the internal rotation of the double rotor H_2O_3 with the conformational processes possible in five membered rings. As one can see from Fig. 11 the H_2O_3 conformations lying in the $-90° < \theta_1, \theta_2 < +90°$ section of the θ_1, θ_2 surface are related to certain ring conformations. For example, the (sp, sp) form is equivalent to the planar five membered ring, the (+og, −og) form to the envelope form, and the (+og, og) form to the twist form. Correspondingly, the inversion of the twist conformation of the ring can be compared with the synchronous disrotatory (inward) rotation of the (og, og) form of H_2O_3. The other conformational process found for five membered rings, namely pseudorotation, resembles the flip-flop rotational mode of H_2O_3. This relationship is illustrated in Fig. 11 where various H_2O_3 conformations are drawn in a way to represent a five membered ring pseudorotating from one (og, −og) form to the other.

It is known that pseudorotation is energetically more favorable than an inversion of the ring.[35] This has to do with the fact that during pseudorotation ring bonds, internal ring angles, and torsional angles periodically vary within certain limits with a phase shift of $\pi/5$ while the inversion process causes a simultaneous change of all parameters taking extreme values in the planar form. We have investigated whether a similar connection applies to the rotational modes of H_2O_3. In Fig. 12, a contour map of the OOO angle α of H_2O_3 is shown. The paths for the flip-flop rotations have been transferred from Fig. 6. Similar plots for the OOH bond angles and the OO bond lengths are given in Figs. 13 and 14.[36] Bond angles and OO bond lengths are coupled to a large degree with the torsional angles θ_1 and θ_2. The contour maps nicely reflect the influence of the two dominating electronic factors. The variation of the bond angles occur in parallel with the changes of the dipole–dipole interactions. This is illustrated by both the direction of the central contour ellipses and the angle minimum in the vicinity of GMIN. The contour map of the OO bond lengths is characterized by a twofold periodicity indicating that the variations of R(OO) are mainly caused by the hyperconjugative effect.

In view of the coupling between structural parameters and rotational angles, the predictions of a rigid rotor

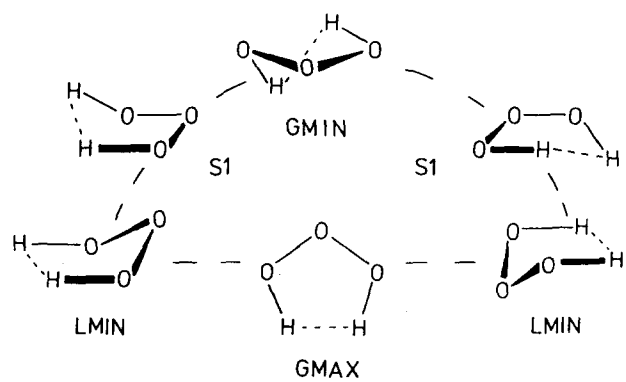

FIG. 11. Illustration of the relationship between a flip-flop rotation of the geminal double rotor H_2O_3 and the pseudorotation of a five membered ring.

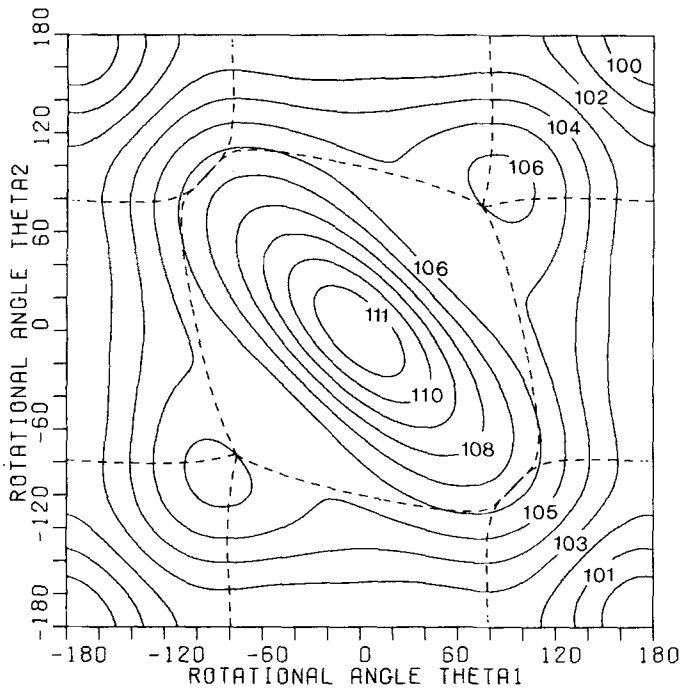

FIG. 12. The variation of the OOO bond angle α as a function of the rotational angles θ_1 and θ_2. Contours are given in degrees. The dashed lines are transferred from Fig. 6.

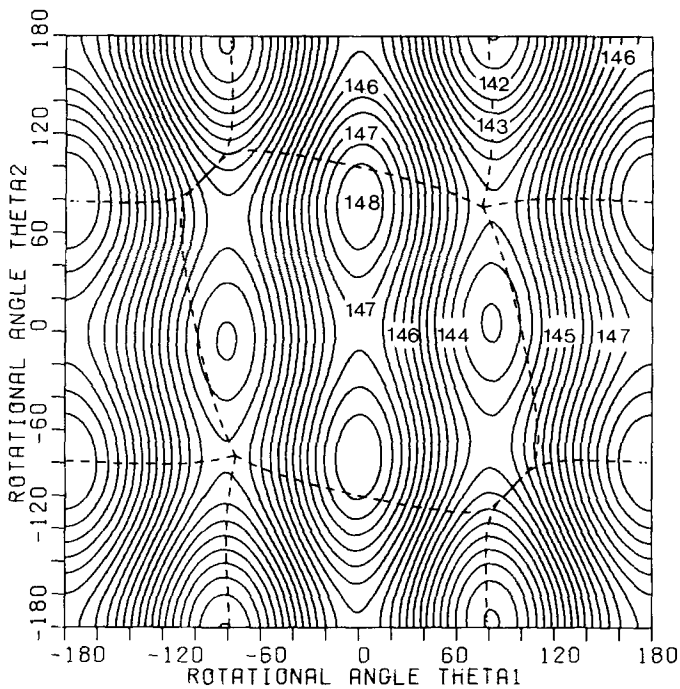

FIG. 14. The variation of the OO bond length as a function of θ_1 and θ_2. Contours are given in picometers. The dashed lines are transferred from Fig. 6.

model seem problematic. However, if one considers only the flip-flop rotational path corresponding to the pseudorotation of a five membered ring, the rigid rotor model has some justification. The variations of the bond angles along the dashed line encircling GMAX amount to less than 2° while those along the "inversion" path (synchronous rotation through the (sp, sp) form) are about four times larger. The OO bonds vary between 144 and 148 pm for both rotational processes. During the flip-flop rotation at least one OO bond length is strengthened. However, the inversion process involves conformations with two unfavorably long OO bond distances. These findings are consistent with the observations made for pseudorotation and stress the relationship of the conformational processes of a geminal double rotor and a five membered ring.

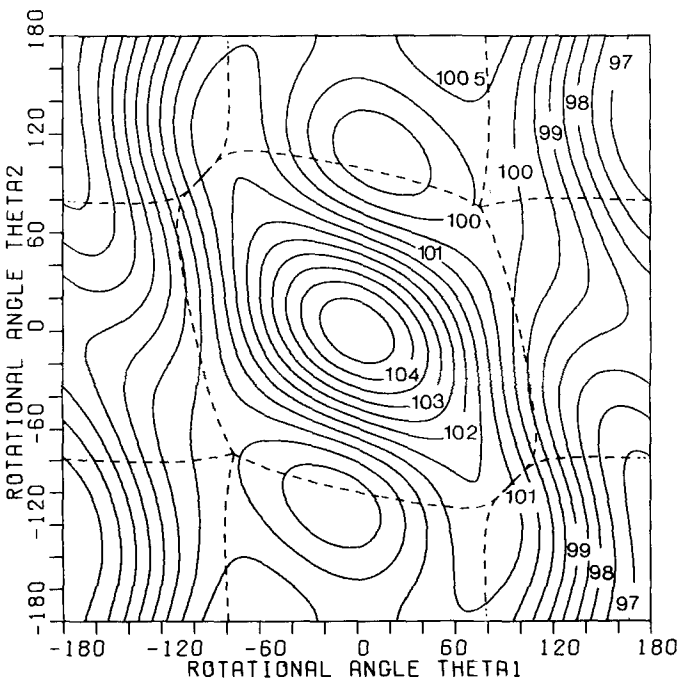

FIG. 13. The variation of the OOH bond angle β as a function of the rotational angles θ_1 and θ_2. Contours are given in degrees. The dashed lines are transferred from Fig. 6.

This relationship suggests using the θ_1, θ_2 surface of H_2O_3 for qualitative predictions concerning the conformational tendencies of 1,2,3-trioxolanes. Apart from the fact that the hydrogens in H_2O_3 are replaced by a CH_2–CH_2 bridge and, hence, the bond polarities are slightly changed, it seems reasonable to expect similar electronic effects for both compounds. At first sight, the twist form of the trioxolane appears to be the conformation of lowest energy since it corresponds to the (sc, sc) form of H_2O_3. This conclusion has also been drawn by Blint and Newton.[9]

A more detailed analysis of the situation is necessary if one recalls that the torsional angles of a puckered five membered ring are considerably smaller than 90°, varying from 0° to 40° around the ring. In the twist (C_2) conformation, the angles θ_1 and θ_2 of the OOO moiety are rather small since the main torsion is around the CC bond. The reverse situation applies to the envelope (C_s) form of 1,2,3-trioxolane. According to inspection of the model, torsional angles θ of about 10° and about 40° seem appropriate for the twist and the envelope forms. Inserting these angle values in the $V(\theta_1, \theta_2)$ potential of H_2O_3 it becomes obvious that the twist form should be less favorable than the envelope form of 1,2,3-trioxolane. The stabilization of the latter is predicted to amount to 6–7 kcal/mole. Probably, this energy differ-

ence will be reduced by ~3 kcal/mole because of unfavorable methylene group eclipsing in the envelope form. Consequently, we predict the envelope form to populate the minima of the conformational surface of 1,2,3-trioxolane which should be characterized by a barrier to pseudorotation of 3–4 kcal/mole. An inversion of the envelope form should require about 7 kcal/mole deduced from the energies of the (sp,sp) form of H_2O_3 (22 kcal/mole) and a skewed form of H_2O_3 (~15 kcal/mole for $\theta_1 = -\theta_2 \approx 40°$). As these predictions are at variance with the calculations of various other authors,[37] a computational verification will be given in the third paper of this series.

IX. H_2O_3—A PROTOTYPE FOR GEMINAL DOUBLE ROTORS

Considering H_2O_3 as a prototype for geminal double rotors one can expect a similar rotational behavior for molecules of the type $X(OY)_2$. In order to verify this assumption we have taken the results of theoretical studies of the internal rotational surface of methanediol[38,39] ($X = CH_2$, $Y = H$), dimethoxymethane[39] ($X = CH_2$, $Y = CH_3$), the phosphate anion[40] ($X = PO_2^-$, $Y = H$), and the dimethyl phosphate anion[41] ($X = PO_2^-$, $Y = CH_3$) from the recent literature. A fit of the conformational energies of these molecules to the Fourier expansion (4) leads to the V_{kl} coefficients listed in Table VII.

According to the computed standard deviations and correlation coefficients, the internal rotational potential of all these molecules is satisfactorily described by expansion (4). The best fit is obtained for the $H_2PO_4^-$ molecule for which we calculate small or vanishing coupling terms V_{11}, V_{22}, and V_{12}. Also, a low dipole effect and a reduced hyperconjugative effect is signified by the values of V_{10} and V_{20}. This finding can be explained by the negative charge associated with the PO_2^- group of the molecule. It opposes the electron withdrawal from the H atoms, thus reducing the OH dipole moments independently from their rotational positions. Accordingly, the dipole–dipole interactions do not play the important role as in the case of H_2O_3. The OH rotors are only weakly coupled which is illustrated by the nearly circular contours of the potential surface. Evidently, the small interactions between the rotating groups explain the success of Kollman's attempt to describe the internal rotational potential of $H_2PO_4^-$ with a small Fourier expansion, including just one coupling term.[40]

For $(CH_3)_2PO_4^-$, the dipole effect and the dipole–dipole interactions seem to have become larger. However, this increase can be caused by the rigid rotor model used for the double rotor.[41] Steric repulsion will be exaggerated in the crowded conformations of the molecule, thus leading to undue charge separations. The large Fourier coefficients of the rigid rotor potential of dimethoxymethane support this interpretation. Therefore, we refrain from a detailed discussion of these values.

In the case of the methanediol, the terms V_{10} and V_{11} nicely reflect the effects of the two basis sets. It is obvious that basis B leads to an exaggeration of the dipole effect which is in line with its tendency to overestimate bond polarities. Contrary to the other rotor molecules studied, the V_{10} coefficient is positive indicating a preference for a *cis* arrangement of bonds in the $HO-CH_2-O$ moiety over a *trans* arrangement. This is consistent with the assumption of two bond dipole moments both directed towards the oxygen atoms, thus being opposed in the *cis* form and reinforcing each other in the *trans* form. Two other conclusions can be drawn from the internal rotational potential of $CH_2(OH)_2$. First, the hyperconjugative effect is rather small which suggests that the interaction between the σ^*_{CO} and $p(O)$ orbitals is not as strong as the corresponding interaction found for H_2O_3. Secondly, the V_{30} term indicates that bond staggering has become more important. The interplay of an increased value of $|V_{30}|$ and the positive sign of V_{10} leads to a shift of the global minimum from the (og,og) form to the (sc,sc) form.

With the aid of the V_{kl} coefficients of Table VII and Eq. (4), we have calculated the exact locations and energies of the saddlepoints of the $CH_2(OH)_2$, $CH_2(OCH_3)_2$, $H_2PO_4^-$ and $(CH_3)_2PO_4^-$ conformational surface. Apart from dimethoxymethane where the available *ab initio* data are not sufficient to describe the complete θ_1, θ_2 potential, we find that the flip-flop rotation of the geminal double rotors proves to be the energetically favored conformational process. The computed barriers are 5.2 (*S*1, Basis B), 4.4 (*S*2, Basis B), 3.8 (*S*1, Basis C), and 3.4 kcal/mole (*S*2, Basis C) for methanediol, 3.2 (*S*1) and 3.3 kcal/mole (*S*2) for the monophosphate anion, and 4.3 (*S*1) and 3.2 kcal/mole (*S*2) for the dimethyl phosphate anion. These barrier heights favorably compete with those of single rotors and underline the conformational flexibility of the double rotors.

X. CONCLUSIONS

The principal conclusions of this work may be summarized as follows:

(1) Accurate calculations on the conformational potential of H_2O_3 require the inclusion of polarization functions in the basis set as well as a complete structure optimization. As in the case of the *trans* barrier of H_2O_2, an insufficient flexibility of the basis leads to an underestimation of the barriers to internal rotation by 1–2 kcal/mole.

(2) Correlation effects have only a small influence on the relative energies of H_2O_3, although the intrapair and interpair contributions vary considerably with the rotational angles. Their low net effect results from an almost complete cancellation over the whole range of the conformational surface which is nicely shown by Fig. 8 and Fig. 9. The influence of correlation decreases if the basis set is improved. Therefore, an accurate recording of the conformational potential of hydrogen trioxide is possible at the HF level of theory.

(3) On the other hand, the determination of the equilibrium structure of H_2O_3 with the HF method appears to be problematic. If the split valence basis B is employed, reasonable structures are calculated. However, this result is fortuitous as it is caused by an overestimation of the bond polarities and an insufficient description of

overlap. Calculations with the augmented basis C provide evidence that the HF method predicts an erroneous equilibrium structure characterized by short OO bond lengths of ~ 139 pm. The inclusion of left–right correlation of electrons in the theoretical model turns out to be mandatory to get a reliable structure of H_2O_3. We note that polarization functions both for the oxygen and the hydrogen atoms become even more important at the RS–MP level than at the HF level of theory.

(4) The conformational behavior of H_2O_3 is dominated by the dipole and the hyperconjugative effect which have also been found to be important for H_2O_2. The relative stabilities of the various H_2O_3 forms can be qualitatively interpreted on the basis of these electronic effects. Their interplay determines the coupling between the OH rotors.

(5) The internal rotational potential is satisfactorily described by the Fourier expansion in Eq. (4). The various V_{kl} terms used in Eq. (4) allow a detailed analysis of the dependence of the electronic effects on the rotational angles. In addition, this potential facilitates the exploration of the internal rotational surface and provides reasonable estimates of the location of the saddlepoints and the steepest descent paths connecting saddlepoint and minimum conformations.

(6) According to the computed energies, the most favorable conversional process of H_2O_3 corresponds to a two-step flip-flop rotation by which the molecules surrounds the energy maxima of the potential surface. We emphasize that the relative energies of the planar H_2O_3 conformations are completely misleading with regard to the rotational flexibility of the molecule. An accurate determination of the barriers to internal rotation of a double rotor demands explicit knowledge of the saddlepoint energies of the potential. In the case of hydrogen trioxide, the actual barriers (6.5 and 5.4 kcal/mole) represent only a fraction of the relative energies of the planar molecular forms which populate the maxima of the rotational surface.

(7) It has been shown that the flip-flop rotation of geminal double rotors is comparable to the pseudorotation of five membered rings. This relationship has been used to predict the conformational tendencies of 1,2,3-trioxolanes. Applying the calculated H_2O_3 potential, we expect the envelope form of the ring to be more stable by 3–4 kcal/mole than the twist form, the latter populating the barrier to pseudorotation. Our prediction is at variance with the results of various other quantum chemical investigations.

(8) We consider H_2O_3 to be a prototype for geminal double rotors of the type $X(OY)_2$. An analysis of the available *ab initio* calculations on methanediol, dimethoxymethane, the monophosphate anion, and its dimethyl derivative supports our view.

ACKNOWLEDGMENTS

This work was supported by the Deutsche Forschungsgemeinschaft. All calculations were carried out at the Cologne Computation Center. The author is grateful to J. Norman of the Cologne Computation Center for his technical advice and to Dr. L. Curtiss of Argonne National Laboratory for fruitful discussions.

[1](a) P. A. Giguère and K. Herman, Can. J. Chem. **48**, 3473 (1970); (b) X. Deglise and P. A. Giguère, Can. J. Chem. **49**, 2242 (1971); (c) P. A. Giguère, Trans. N. Y. Acad. Sci. **34**, 334 (1972); (d) J. L. Arnau and P. A. Giguère, J. Chem. Phys. **60**, 270 (1974); (e) G. Czapski and B. H. J. Belsi, J. Phys. Chem. **67**, 2180 (1963); **72**, 3836 (1968).
[2]P. D. Bartlett and M. Lahav, Isr. J. Chem. **10**, 101 (1972).
[3](a) R. P. Hirschmann, W. B. Fox, and L. R. Anderson, Spectrochim. Acta **25**, 811 (1969); (b) J. D. Witt, J. R. Durig, D. Des Marteau, and R. M. Hammaker, Inorg. Chem. **12**, 807 (1973); (c) F. A. Hohorst, D. Des Marteau, L. R. Anderson, D. E. Gould, and W. B. Fox, J. Am. Chem. Soc. **95**, 2657 (1973).
[4]N. Youeda and G. A. Olah, J. Am. Chem. Soc. **99**, 3113 (1977).
[5]See, e.g., F. E. Stary, D. E. Emge, and R. W. Murray, J. Am. Chem. Soc. **98**, 1880 (1976), and references, therein.
[6](a) R. U. Lemieux, in *Molecular Rearrangements* Part 2, edited by P. De Mayo (Interscience, New York, 1964), p. 723; (b) E. L. Eliel, Angew. Chem. **84**, 779 (1972).
[7](a) R. Criegee, Rec. Chem. Prog. **18**, 111 (1957); (b) N. L. Bauld, J. A. Thompson, C. E. Hudson, and P. S. Bailey, J. Am. Chem. Soc. **90**, 1822 (1968). For a recent review see (c) R. Criegee, Angew. Chem. **87**, 765 (1975).
[8](a) L. Radom, W. J. Hehre, and J. A. Pople, J. Chem. Soc. A **1971**, 2299 (1971); (b) L. Radom, W. J. Hehre, and J. A. Pople, J. Am. Chem. Soc. **93**, 289 (1971).
[9]R. J. Blint and M. D. Newton, J. Chem. Phys. **59**, 6220 (1973).
[10](a) B. Plesničar, S. Kaiser, and A. Ažman, J. Am. Chem. Soc. **95**, 5476 (1973); see also (b) B. Plesničar, D. Kocjan, S. Murovec, and A. Ažman, J. Am. Chem. Soc. **98**, 3143 (1976).
[11](a) C. C. J. Roothaan, Rev. Mod. Phys. **23**, 69 (1951); (b) G. G. Hall, Proc. Roy. Soc. London Ser. A **205**, 541 (1951).
[12](a) T. H. Dunning, Jr., J. Chem. Phys. **53**, 2823 (1970); (b) T. H. Dunning, Jr., J. Chem. Phys. **55**, 3958 (1971).
[13]W. J. Hehre, R. F. Stewart, and J. A. Pople, J. Chem. Phys. **51**, 2657 (1969).
[14]R. Ditchfield, W. J. Hehre, and J. A. Pople, J. Chem. Phys. **54**, 724 (1971).
[15]P. C. Hariharan and J. A. Pople, Theoret. Chim. Acta **28**, 213 (1973).
[16]C. Møller and M. S. Plesset, Phys. Rev. **46**, 618 (1934).
[17]D. Cremer, (to be published).
[18]W. J. Hehre, W. A. Lathan, R. Ditchfield, M. D. Newton, and J. A. Pople, Program No. 236, Quantum Chemistry Program Exchange, University of Indiana.
[19]D. Cremer, 11. Symposium der Theoretischen Chemie, Bad Boll (1975).
[20]Similar conclusions can also be drawn if the electronic structure of ozone is considered. Ozone is a diradical with a weak π-bond between the two terminal atoms. [See, e.g., W. A. Goddard, III, T. H. Dunning, Jr., W. J. Hunt, and P. J. Hay, Acc. Chem. Res. **6**, 368 (1973)]. Thus, the H atoms in H_2O_3 would be expected to be bonded on the terminal O atoms, in a plane perpendicular to the O_3 groups.
[21](a) M. J. S. Dewar, *The Molecular Orbital Theory of Organic Chemistry* (McGraw-Hill, New York, 1969); (b) L. Salem, J. Am. Chem. Soc. **90**, 543 (1968); (c) K. Fukui, Acc. Chem. Res. **4**, 57 (1971); (d) N. D. Epiotis, W. R. Cherry, S. Shaik, R. Yates, and F. Bernardi, "Structural Theory of Organic Chemistry," Top. Curr. Chem. **70**, 1 (1977).
[22]In the case of the interaction of a doubly occupied orbital $\varnothing_i$ and a singly occupied orbital $\varnothing_j(\varnothing_9-\varnothing_4'; \varnothing_8-\varnothing_5')$ it has been as-

sumed that the π-like overlap is smaller than 0.33. Under this condition, the interaction is stabilizing. See (a) R. F. Hudson, Angew. Chem. **85**, 63 (1973); (b) F. Bernardi, N. D. Epiotis, W. Cherry, H. B. Schlegel, M-H. Whangbo, and S. Wolfe, J. Am. Chem. Soc. **98**, 469 (1976).

[23]Paper I, D. Cremer, J. Chem. Phys. **69**, 4440 (1978).

[24]Equation (1), of course, represents the energy of interaction between two ideal dipoles ($r_{ab} \gg l$) which significantly deviates from the value of (1) if real dipoles are considered ($r_{ab} \sim l$). See, for example, J. O. Hirschfelder, C. F. Curtiss, and R. B. Bird, *Molecular Theory of Gases and Liquids* (Wiley, New York, 1964), Chap. 12.

[25]C. Romers, C. Altona, H. R. Buys, and E. Havinga, in *Topics in Stereochemistry*, Vol. 41, edited by E. L. Eliel and N. L. Allinger (Wiley-Interscience, New York, 1969), p. 39.

[26]L. Radom, W. J. Hehre, and J. A. Pople, J. Am. Chem. Soc. **94**, 2371 (1972).

[27]E. L. Eliel, N. L. Allinger, S. J. Angyal, and G. A. Morrison, *Conformational Analysis* (Wiley, New York, 1965).

[28]D. Cremer, J. S. Binkley, J. A. Pople, and W. J. Hehre, J. Am. Chem. Soc. **96**, 6900 (1974).

[29]The structures of a variety of two and three-heavy atom molecules have been evaluated at the RHF and RS–MP level of theory with augmented basis sets. The RHF bond lengths are consistently found to be too short with regard to experimental values while the RS–MP values are in agreement with observed bond lengths. D. Cremer, (to be published).

[30]D. Cremer and D. Christen, J. Mol. Spectrosc. (submitted for publication).

[31]The standard deviation is defined by $\sigma = (\sum_{i=1}^{N} (E(\theta_1, \theta_2) - V(\theta_1, \theta_2))^2/(N-M))^{1/2}$ where N *ab initio* energies are used to determine M Fourier coefficients V_{kl}. The square of the correlation coefficient r is given rather than r itself because r^2 provides a better descriptive measure.

[32]The form of the V_{k0} terms has been chosen according to the convention used for single rotors.

[33]The $\cos(\theta_1 + \theta_2)$ term remains constant for $\theta_1 = -\theta_2$, but it varies for $\theta_1 = \theta_2$ which is appropriate since the largest change in energies occurs along the line $\theta_1 = \theta_2$. A dissection into a sine and a cosine part has the advantage that a variation of energies is induced along both diagonals. The same holds for the inclusion of the sine parts in the V_{12} term.

[34]There are only four $S2$ saddlepoints within the range $-180° \leq \theta_1, \theta_2 \leq 180°$. (See values of θ_1 and θ_2 in Tables II and V.) The steepest ascent and descent paths to and from one of the eight saddlepoints have been calculated by means of Eq. (4).

[35]D. Cremer and J. A. Pople, J. Am. Chem. Soc. **97**, 1358 (1975), and references cited therein.

[36]The dependence of R(OO) and β(OOH) on θ_1 and θ_2 has been calculated with expansion (4) by decoupling the Fourier components combined in V_{10}, V_{20}, V_{30}, and V_{12}.

[37](a) J. Renard and S. Fliszár, J. Am. Chem. Soc. **92**, 2629 (1970); (b) S. Fliszár, J. Renard, and D. Z. Simon, **93**, 6953 (1971); (c) R. A. Rouse, **95**, 3460 (1973).

[38]G. A. Jeffrey, J. A. Pople, and L. Radom, Carbohydr. Res. **25**, 117 (1972).

[39]G. A. Jeffrey, J. A. Pople, J. S. Binkley, and S. Vishveshwara, J. Am. Chem. Soc. **100**, 373 (1978).

[40]D. M. Hayes, P. A. Kollman, and S. Rothenberg, J. Am. Soc. **99**, 2150 (1977).

[41]M. D. Newton, J. Am. Chem. Soc. **95**, 256 (1973).